



## Rhenium(I)-based fluorescence resonance energy transfer probe for conformational changes of bovine serum albumin

Jayaraman Bhuvaneshwari, Ayub Khan Fathima, Seenivasan Rajagopal\*

School of Chemistry, Madurai Kamaraj University, Madurai 625 021, India

### ARTICLE INFO

#### Article history:

Received 13 April 2011

Received in revised form 5 October 2011

Accepted 27 October 2011

Available online 4 November 2011

#### Keywords:

Rhenium(I) tricarbonyl complex

Bovine serum albumin

Energy transfer

Protein binding

### ABSTRACT

Protein binding properties of *fac*-rhenium(I) complexes with general structure  $[\text{Re}(\text{CO})_3(\text{N-N})\text{L}]\text{PF}_6$ , where N-N = 4,4'-dianoyl-2,2'-bipyridine and L = py-3-COOH (**1a**) and py-3-CONH<sub>2</sub> (**1b**) with bovine serum albumin (BSA) were investigated at physiological pH (7.4) using UV–visible absorption and fluorescence spectral study, excited state lifetime measurement and circular dichroism (CD). The results observed from fluorescence spectra reveal the energy transfer from BSA to Re(I) complex, and the distance *r* between donor (BSA) and acceptor (Re(I) complex) is 3.05 nm and 2.16 nm for **1a** and **1b** respectively according to Forster's non-radiative energy transfer theory. CD results show that the binding of Re(I) complex could induce the conformational change with the loss of  $\alpha$ -helicity.

© 2011 Elsevier B.V. All rights reserved.

### 1. Introduction

The use of Re(I)-based luminophores has attracted significant attention due to the favorable photophysical properties associated with complexes of the generic form *fac*- $[\text{Re}(\text{CO})_3(\text{N-N})(\text{L})]^+$  (where L = monodentate and N-N = bidentate ligands) [1–7]. Since the excited state is formally localized on the single diimine ligand (Metal to Ligand Charge Transfer (MLCT), Re → N-N), these complexes often serve as more sensitive probes than related trischelated  $[\text{Ru}(\text{diimine})_3]^{2+}$  complexes [8]. This advantage leads to the development of a variety of Re(I) derived systems exploited in cellular imaging using fluorescence microscopy [9]. Schanze et al. [10] and Yam et al. [11] reported the luminescent properties of Re(I)-anthracene system and its application as a luminescent probe for DNA binding. Coogan et al. [12] used Re(I) complex for cell imaging.

The development of transition metal complexes that target and interact non-covalently with proteins is an emerging field that links bioinorganic chemistry with chemical and synthetic biology [3,13–15]. The metal complexes are very much suited to the optimization of non-covalent interactions, since they combine flexibility in ligand design with access to a variety of coordination geometries, oxidation states and electronic configurations [16]. Once protein is bound to a metal ion, metal ion plays a structural role, particularly on protein folding, but can also determine the reactivity of a protein as part of redox or catalytic

center site [17]. Shahabadi and Maghsudi studied the interaction between Cu(II) complexes and BSA using absorption, fluorescence and circular dichroism spectroscopy [18]. Palaniandavar et al. reported the cleavage of BSA using Cu(II) phenolate complex [19]. Recently Lo et al. extensively studied the protein binding properties of Re(I) complexes with BSA [20,21]. In this perspective, we report our results obtained through the study of interaction of Re(I)-complexes carrying hydrophobic ligand with protein *via* non-covalent interactions to design spectroscopic probes.

BSA belongs to a class of proteins most widely studied category and functions as a carrier for many fatty acid anions and other simple amphiphiles in a blood stream [22]. It has a molecular weight of  $6.8 \times 10^4 \text{ g mol}^{-1}$  and contains 583 amino acids in a single polypeptide chain. The protein contains 17 disulfide bridges and one free-SH group, which can cause it to form a covalently linked dimer. The interior of the protein is almost hydrophobic, while both the charged amino acid residues and apolar patches cover the interface. The tertiary structure of BSA is composed of three domains I–III and each domain consist two subdomains A and B. Because of the common interface between domains II and III, binding of a probe to domain III is associated with the conformational changes of domain II and hence its binding affinities. BSA contains two tryptophan residues, Trp-134 and Trp-212, of which the former is located in hydrophilic subdomain 1B, and it is proposed to be located near the surface of albumin molecule in the second helix of the first domain. Trp 212 is located within a hydrophobic binding pocket of the protein. BSA is known to exhibit a very high conformational adaptability to a large variety of ligands [22,23]. In general BSA has been used extensively in the past years, partly because of its structural homology with HSA [24,25]. In this work, we report

\* Corresponding author. Tel.: +91 452 2458246.

E-mail address: [rajagopalseenivasan@yahoo.com](mailto:rajagopalseenivasan@yahoo.com) (S. Rajagopal).

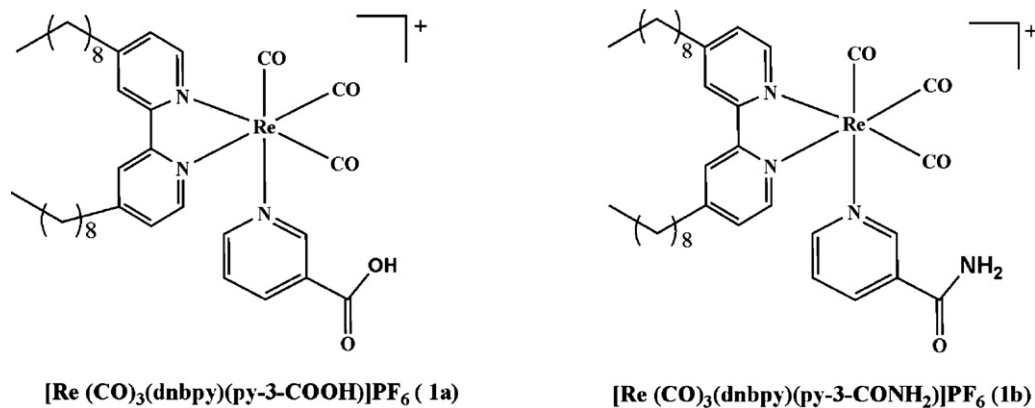


Chart 1. Structure of the rhenium(I) complexes.

the protein (BSA) binding properties of Re(I) complexes carrying surfactant ligands. The interaction of proteins with surfactants has received a great deal of interest for many years due to its application in a great variety of industrial, biological and cosmetics system [26,27].

## 2. Experimental

### 2.1. Materials

The chemicals used in this study  $\text{Re}_2(\text{CO})_{10}$  and ligands 4,4'-dinanoyl-2,2'-bipyridine (dnbpy), nicotinic acid (py-3-COOH) and nicotinamide (py-3-CONH<sub>2</sub>) were obtained from Aldrich and Merck and used as such. BSA was purchased from Genei.  $\text{Re}(\text{CO})_5\text{Br}$  was obtained by the oxidative addition of  $\text{Br}_2$  to  $\text{Re}_2\text{CO}_{10}$  [28].

### 2.2. Synthesis of Re(I) complexes

The complexes  $[\text{Re}(\text{N-N})(\text{CO})_3(\text{L})]\text{PF}_6$  (N-N = dnbpy and L = py-3-COOH or py-3-CONH<sub>2</sub>) were prepared from  $\text{Re}(\text{CO})_5\text{Br}$  by the modification of the method reported by Lo et al. [29] (see Supporting Information).

### 2.3. Instrumentation and methods

The stock solution of BSA ( $1 \times 10^{-3}$  M) based on its molecular weight of 68,000 was prepared in buffer solution at physiological pH (7.4). The stock solution for complexes **1a** and **1b** ( $1 \times 10^{-3}$  M) were prepared in acetonitrile (HPLC). Double distilled water was used throughout the experiment. The sample solutions were prepared freshly for each measurement.

The Re(I) complexes were characterized using mass, NMR and IR techniques. The mass spectra were recorded using a Quattro LC triple-quadrupole mass spectrometer (Micromass, Manchester, UK) interfaced to an ESI (Electro Spray Ionization) source; data acquisition was done under the control of Masslynx software (version 3.2), the ESI capillary voltage was maintained between 4.0 and 4.2 kV and the cone voltage kept at 25 V. Nitrogen was used as desolvation and nebulization gas. NMR spectra were recorded on Bruker (300 MHz) spectrometer and IR spectra using 8400S Shimadzu-FT-IR spectrophotometer.

Absorption spectra were recorded using Analytik Jena Specord S100 spectrometer. The emission was recorded using Varian Cary Eclipse spectrofluorometer. All the sample solutions used for the emission measurements were deaerated for about 30 min, by dry  $\text{N}_2$  purging by keeping solution in cold water to ensure that there is no change in the volume of the solution. All the measurements were done at room temperature. Both the absorption and emission

titrations were carried out by keeping the concentration of BSA as constant ( $1 \times 10^{-5}$  M) while varying the concentration of complexes (**1a** and **1b**) from 0  $\mu\text{M}$  to 24  $\mu\text{M}$ .

The fluorescence measurements were performed at different concentrations of Re(I) complexes and the quenching rate constant,  $k_q$ , values were determined from the modified Stern-Volmer plot using the Eq. (1) [30].

$$\frac{F_0}{F_0 - F} = \frac{1}{fK[Q]} + \frac{1}{f} \quad (1)$$

where  $F_0$  is the initial fluorescence intensity and  $F$  is the fluorescence intensity in the presence of quenching agent or interacting molecule (Re(I) complex).  $K$  is the Stern-Volmer quenching constant,  $[Q]$  is the molar concentration of quencher (Re(I) complex), and  $f$  is the fraction of accessible fluorophore-quencher complex, which indicates the fractional fluorescence contribution of the total emission for an interaction with a hydrophobic quencher [31]. The plot of  $F_0/(F_0 - F)$  vs  $1/[Q]$  yields  $f^{-1}$  as the intercept on the y axis and  $(fK)^{-1}$  as the slope.  $k_q$ , the quenching rate constant is calculated from obtained  $K$  value.

Time resolved fluorescence measurements were carried out using a diode laser-based time correlated single photon counting (TCSPC) spectrometer from IBH, UK. In the present study, a 295 nm diode laser (50 kHz) was used as the excitation source and Hamamatsu photomultiplier tube was used for the fluorescence detection. The instrument response function for this system is  $\approx 1.2$  ns and the fluorescence decay was analyzed using the software provided by IBH (DAS-6) and PTI global analysis software.

Circular dichroism (CD) measurements were performed on a JASCO J810 spectropolarimeter at RT over the wavelength 200–260 nm. Parameters were set as follows: path length, 50 mm; resolution, 0.5 nm; scan speed, 50 nm min<sup>-1</sup>; band width, 1 nm; response 1 s. Every spectrum was averaged two times. The concentration of BSA is  $3 \times 10^{-6}$  M and the concentration of Re(I) complex is  $1 \times 10^{-5}$  M.

## 3. Results and discussion

The structure of the Re(I) complexes synthesized for the present study are shown in Chart 1. The absorption and emission spectra of **1a** in acetonitrile are shown in Fig. 1 and the spectral data of Re(I) complexes are collected in Table 1. The electronic absorption spectra of Re(I)-tricarbonyl complexes **1a** and **1b** reveal strong absorption bands at 225–315 nm and less intense absorption shoulders at 345–360 nm. With reference to previous studies on related Re(I) complexes [32–34], these strong high energy absorption bands at 225–315 nm are assigned to ligand centered (LC)  $\pi$ - $\pi^*$  transition and low energy absorption shoulders at 345–360 nm

**Table 1**  
Photophysical properties of the Re(I)-complexes in CH<sub>3</sub>CN and IR spectral data.

Complex	$\lambda_{\text{abs}}$ , nm ( $\epsilon_{\text{max}}$ , dm <sup>3</sup> mol <sup>-1</sup> cm <sup>-1</sup> )	$\lambda_{\text{em}}$ (nm)	$\tau$ (ns)	$\nu(\text{CO})$ (cm <sup>-1</sup> )
Re-dnbpy-Br	216 (29,236), 245 (19,547), 288 (14,308), 369 (3461)	587	46	2019, 1915, 1890
<b>1a</b>	222 (31,995), 246 (26,964), 274 (23,059), 310 (16,230), 349 (5930)	549	138	2029, 1911
<b>1b</b>	219 (32,757), 239 (27,398), 269 (25,343), 305 (17,769), 360 (9854)	538	123	2027, 1905
BSA	278 (45,110)	348	–	–

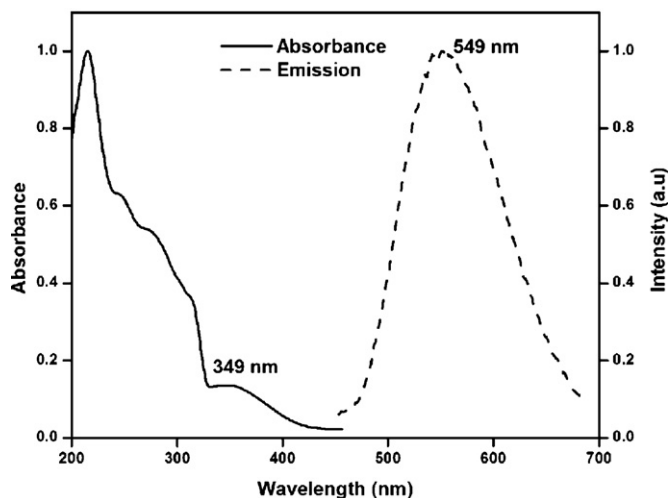


Fig. 1. Normalized absorption and emission spectra of complex **1a** in acetonitrile.

to spin allowed metal-to-ligand charge transfer (<sup>1</sup>MLCT) transition from the Re d $\pi$ -orbital to the  $\pi^*$  orbital of the ligand d $\pi$  Re  $\rightarrow \pi^*$  (diimine). Complexes **1a** and **1b** show luminescence in the region 545–555 nm in acetonitrile at RT. Variation in the axial ligand (replacement of Br with py-3-COOH and py-3-CONH<sub>2</sub>) shifts the MLCT emission to higher energies (shorter wavelengths) due to the stabilization of the Re d $\pi$ -orbitals.

### 3.1. Steady state absorption and emission spectra

Fig. 2 shows the absorption spectrum of BSA in the absence and in the presence of complex **1b**. The absorption spectrum of BSA shows a maximum at 280 nm, which is characteristic absorption of

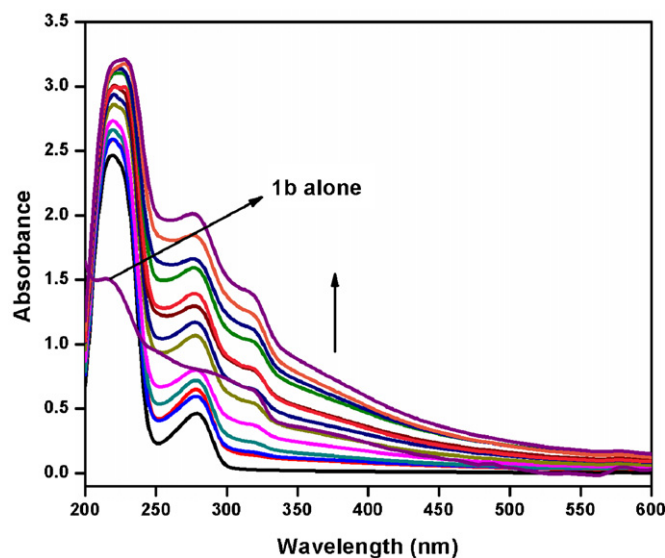


Fig. 2. Absorption spectra of BSA ( $1 \times 10^{-5}$  M) in the absence and presence of different concentration of complex **1b** ( $[1b] = 0 \rightarrow 24 \mu\text{M}$ ).

tryptophan (Trp) and tyrosine (Tyr) residues in proteins [35]. The interesting point to be noted here is that in the absence of BSA the absorption intensity of **1b** ( $[1b] = 24 \mu\text{M}$ ) at 318 and 360 nm are 0.64 and 0.33, respectively. But on the addition of BSA, the intensity of these bands increased up to 1.41 and 0.81. This is the first spectral evidence towards the occurrence of interaction between BSA and Re(I) complex.

Generally, the fluorescence of protein is caused by three intrinsic fluorophores present in protein, i.e., Trp, Tyr and phenylalanine (Phe) residues [18]. Actually, the intrinsic fluorescence of many proteins is mainly contributed by tryptophan alone because of very low quantum yield of Phe, and the fluorescence of Tyr is almost quenched *via* energy transfer to Trp if Tyr is ionized, near an amino or carboxyl group. In order to confirm the interaction between Re(I) complexes and BSA, fluorescence titration is also carried out for the same sample solutions used for the absorption measurements. The result of interaction of Re(I) complex with BSA is found to produce dramatic modifications on the emission profile of both BSA (Fig. 3A) and Re(I) complex (Fig. 3B). The fluorescence of BSA is quenched in the presence of Re(I) complex with a blue shift ( $\approx 10$  nm) in the emission maximum. The variation in the tryptophan emission is the consequence of the protein conformational changes. The mixing of BSA with complex **1b** induces an enhancement along with blue shift ( $\approx 540 \rightarrow 525$  nm) (Fig. 3B) in the luminescence of Re(I) complex (the same trend is observed for complex **1a**, blue shift from  $\approx 550 \rightarrow 535$  nm, see Supporting Information). We propose that the major force for these spectral changes is the strong hydrophobic interaction between Re(I) complex and BSA. Tajmir-Riahi et al. [30] and Guchhait et al. [36] observed the similar results for polyphenols and 5-(4-dimethylamino-phenyl)-penta-2,4-dienoic acid methyl ester (DPDAME) in the presence of BSA. The fluorescence quenching of BSA in addition to blue shift in the emission maximum suggests that binding of Re(I) complex is associated with the change in the environment of at least one of the two Trp moieties in BSA. The binding constant ( $K_b$ ) of BSA with Re(I)-complexes is determined using Eq. (2) [30]

$$\log \left[ \frac{F_0 - F}{F} \right] = \log K_b + n \log [Q] \quad (2)$$

where  $F_0$  and  $F$  are the fluorescence intensities of BSA before and after the addition of Re(I) complex,  $n$  is the number of binding sites and  $[Q]$  is the concentration of Re(I) complex. The obtained binding constant values are collected in Table 2. The binding constants are  $7.3 \times 10^5 \text{ M}^{-1}$  and  $5.6 \times 10^6 \text{ M}^{-1}$  for **1a** and **1b**, respectively. This large binding constants indicate that there is a strong interaction between BSA and Re(I)-complex.

Fig. 4 shows the modified Stern-Volmer plot for the quenching of BSA with complex **1b** and the  $K_{SV}$  values are  $1.5 \times 10^4 \text{ M}^{-1}$  and  $2.0 \times 10^4 \text{ M}^{-1}$  for complexes **1a** and **1b**, respectively. The calculated  $k_q$  values are  $2.6 \times 10^{12} \text{ dm}^3 \text{ mol}^{-1} \text{ s}^{-1}$  and  $3.5 \times 10^{12} \text{ dm}^3 \text{ mol}^{-1} \text{ s}^{-1}$  for complexes **1a** and **1b**, respectively (Table 2). In general, the maximum collision quenching constant ( $k_q$ ) of various kinds of quenchers to biopolymers is  $2.0 \times 10^{10} \text{ L mol}^{-1} \text{ s}^{-1}$  [37]. Obviously, the quenching rate constant of BSA-Re(I) system is very high compared to the collisional quenching constant of biopolymer. This shows that the major component of quenching of BSA by Re(I) complex is *via* the formation of complex between BSA and Re(I) ion i.e., the major contribution

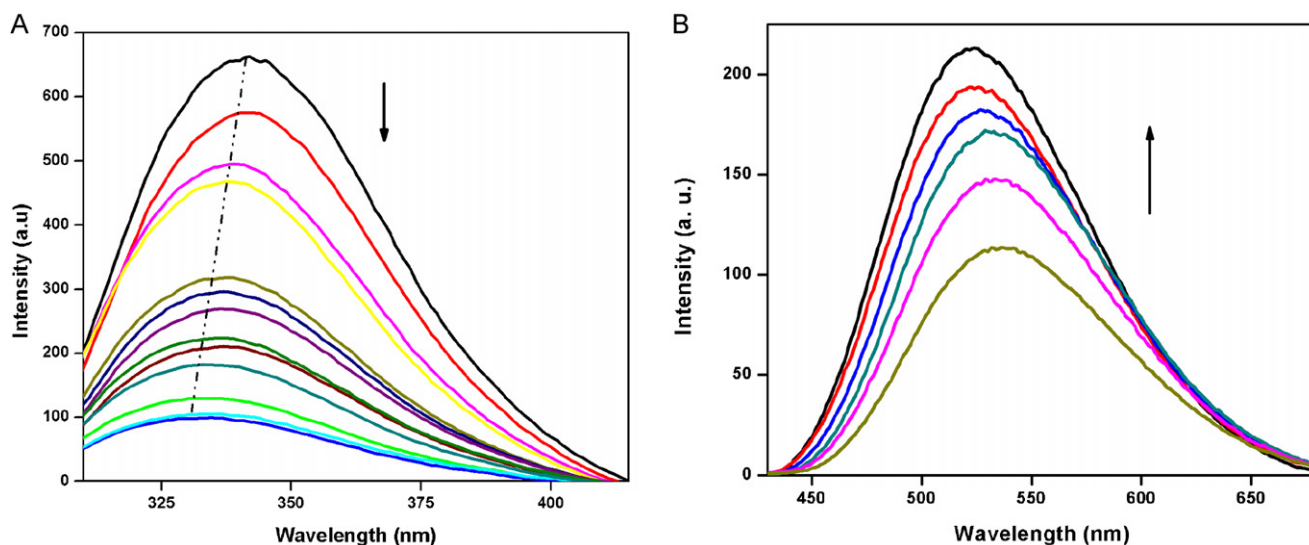


**Fig. 3.** (A) Fluorescence quenching of BSA in the presence of various **1b** ( $0 \rightarrow 24 \mu\text{M}$ ),  $[\text{BSA}] = 1 \times 10^{-5} \text{ M}$  excitation maximum – 290 nm; (B) fluorescence enhancement of complex **1b** in the presence of various  $[\text{BSA}]$  ( $0 \rightarrow 100 \mu\text{M}$ ),  $[\text{1b}] = 1 \times 10^{-5} \text{ M}$  excitation maximum – 360 nm.

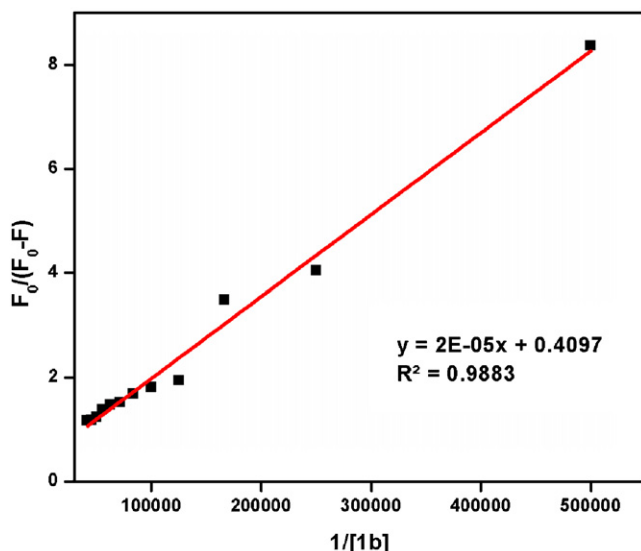


**Fig. 4.** Stern-Volmer plot for the quenching of BSA with complex **1b**.

for the BSA fluorescence quenching with Re(I)-complex is the static quenching process.

### 3.2. Fluorescence resonance energy transfer (FRET)

The past few years, in the field of photochemistry and photobiology, have witnessed an awesome progression of research

related to the photophysical studies on metal complexes bound to biomolecules particularly on fluorescence resonance energy transfer in the donor (D)–acceptor (A) prototype [38–41]. During the FRET process, the donor emission intensity is found to be decreased with concomitant increase in the acceptor emission intensity as the acceptor concentration increases. It is interesting to note that the quenching of fluorescence of BSA accompanies simultaneous increase in the intensity of a new band at  $\approx 535 \text{ nm}$  (Fig. 5A) for both complexes **1a** and **1b** which is the CT emission of Re(I) complex (blue shifted from  $555 \rightarrow 532 \text{ nm}$  for complex **1a** and  $540 \rightarrow 535 \text{ nm}$  for complex **1b** with  $[\text{BSA}] = 1 \times 10^{-5} \text{ M}$ ). Interestingly, we have observed the luminescence enhancement of Re(I) complex on the addition of BSA at constant  $[\text{Re(I) complex}]$  (Fig. 3B). The blue shift in the fluorescence maximum of BSA in the presence of Re(I) complex and luminescence enhancement of Re(I) complex in the presence of BSA (Fig. 3) can be rationalized on the basis of the modification of the local environments of the Trp residue as well as Re(I) complex during the interaction between BSA and Re(I) complex. In addition, the clear isoemissive point at 415 nm (Fig. 5A) indicates that the quenching of the fluorescence of BSA depends on the formation of BSA–Re(I) complex [42]. Taking into account an overlap between the emission spectrum of BSA and the absorption spectrum of Re(I) complex (Fig. 5B), an excited state energy transfer mechanism may be proposed.

The importance of FRET in biochemistry is that the efficiency of transfer can be used to evaluate the distance,  $r$ , between the probe (Re(I)-complex) and Trp residue in the protein. According to the Forster's non-radiative energy transfer theory [43], the rate of energy transfer depends on (i) the relative orientation of the donor (BSA) and the acceptor (Re(I) complexes) dipoles, (ii) the extent of

**Table 2**

Binding constant ( $K_b$ ), quenching constant ( $k_q$ ) and lifetime ( $\tau$ ) data for BSA in the presence of Re(I) complexes.

Complex	$K_b$ ( $\text{M}^{-1}$ )	$n$	$k_q$ ( $\text{dm}^3 \text{ mol}^{-1} \text{ s}^{-1}$ )	$\tau_1$ , ns (%)	$\tau_2$ , ns (%)	$\chi^2$
<b>1a</b>	$7.3 \times 10^5 \pm 0.1$	1.2	$2.6 \times 10^{12}$	–	–	–
<b>1b</b>	$5.6 \times 10^6 \pm 0.2$	1.3	$3.5 \times 10^{12}$	–	–	–
BSA <sup>a</sup>	–	–	–	1.32 (8.32)	5.85 (91.68)	1.20
BSA + 10 $\mu\text{M}$ <b>1a</b>	–	–	–	0.96 (8.57)	5.44 (91.43)	0.99
BSA + 20 $\mu\text{M}$ <b>1a</b>	–	–	–	0.24 (13.41)	5.21 (86.59)	1.05
BSA + 10 $\mu\text{M}$ <b>1b</b>	–	–	–	0.60 (12.52)	5.16 (87.48)	1.07
BSA + 20 $\mu\text{M}$ <b>1b</b>	–	–	–	0.11 (17.52)	4.94 (82.96)	1.02

<sup>a</sup>  $[\text{BSA}] = 1 \times 10^{-5} \text{ M}$ .

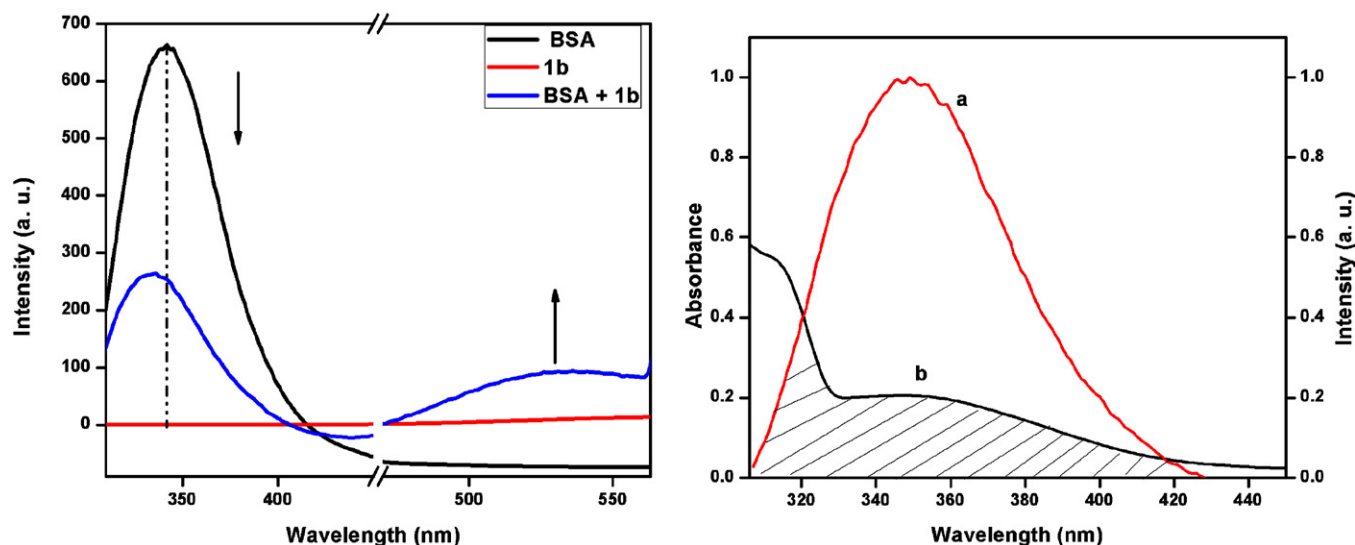


Fig. 5. Overlap between the emission spectrum of BSA (a) and the absorption spectrum of Re(I) complex (b) (right). Fluorescence resonance energy transfer (FRET) from BSA to bound Re(I) complex ( $[BSA] = 10 \mu\text{M}$ ,  $[1b] = 10 \mu\text{M}$ ) (left), excitation maximum – 290 nm.

overlap of emission spectrum of the donor with absorption spectrum of the acceptor and (iii) the distance between the donor and the acceptor. The efficiency of energy transfer,  $E$ , is calculated using Eq. (3).

$$E = 1 - \frac{F}{F_0} = \frac{R_0^6}{R_0^6 + r^6} \quad (3)$$

where  $F$  and  $F_0$  are the fluorescence intensities of BSA in the presence and absence of Re(I) complex ( $24 \mu\text{M}$ ),  $r$  is the distance between the acceptor and the donor and  $R_0$  is the critical distance when the transfer efficiency is 50% and the value is given by Eq. (4).

$$R_0^6 = 8.79 \times 10^{-25} \chi^2 n^{-4} \phi J \quad (4)$$

$$J = \frac{\sum F(\lambda) \varepsilon(\lambda) \lambda^4 \Delta \lambda}{\sum F(\lambda) \Delta \lambda} \quad (5)$$

Here  $F(\lambda)$  is the fluorescence intensity of the fluorescent donor at the wavelength  $\lambda$  and  $\varepsilon(\lambda)$  the molar absorption coefficient of the acceptor at  $\lambda$ . The value of  $J$  is  $6.6 \times 10^{-14} \text{ cm}^{-1} \text{ M}^{-1}$  and  $1.4 \times 10^{-14} \text{ cm}^{-1}$  for **1a** and **1b**, respectively, which is calculated by integrating the spectra collected in Fig. 5B. It has been reported for BSA that  $K^2 = 2/3$ ,  $\phi = 0.15$ , and  $N = 1.336$  [44]. Based on these data, we estimated  $R_0$  and  $r$  values and the data are collected in Table 3. The donor to acceptor distance,  $r < 8 \text{ nm}$  indicates that the energy transfer from BSA to Re(I)-complex occurs with high possibility [45]. That is the donor (tryptophan of BSA) and acceptor (Re(I)) can approach very close for very high energy transfer efficiency. This also indicates that the probe can measure the proteinous microenvironment at a distance of 3.05 and 2.16 nm. As far as we know, it seems to be the first documentation of energy transfer from BSA to Re(I) complex. That the ratio  $r/R_0$  amounts to 0.87 and 0.80 for complex **1a** and **1b**, respectively, i.e., within the range 0.5–2.0, rationalizes the practical reliability of the FRET process to measure the

distance between donor and acceptor chromophore in the present case [31].

### 3.3. Lifetime measurement

Time-resolved fluorescence study is also carried out to investigate the quenching mechanism of BSA fluorescence by Re(I) complexes **1a** and **1b**. Fluorescence lifetime serves as a sensitive parameter for exploring the local environment around a fluorophore, and it is sensitive to excited-state interactions [46]. It also contributes to the understanding of the interactions between the probes and the proteins [47]. The fluorescence lifetime of the tryptophan residues in proteins is a complex function of its interactions with the local environment and the solvent. The fluorescence decay curves were fitted to biexponential function with acceptable  $\chi^2$  values (Table 2) for BSA in the absence and presence of probe. The literature data show that native BSA has two lifetime components: one ( $\tau_1 = 5.85 \pm 0.2 \text{ ns}$ ) contributing 75% of the total fluorescence, and the other ( $\tau_2 = 1.2 \pm 0.2 \text{ ns}$ ) contributing the rest of the fluorescence [48]. The one with a longer lifetime is assigned to Trp-134 (hydrophilic in nature), and the other to Trp-212 (hydrophobic in nature) [30,36]. The relative contribution of each component is dependent on the folding/unfolding conditions due to the protein's multiple local configurations and changes in the extent of solvent accessibility [49]. Fig. 6 shows the decrease in the  $\tau$  value of BSA with increasing the probe concentration. The lifetime of BSA alone in buffer is 5.85 ns and 1.32 ns, which are in good agreement with the reported values [49]. A glance at Table 2 and Fig. 6 reflect that two lifetime values observed,  $\tau_1$  and  $\tau_2$ , decrease in the presence of the Re(I) complexes than those measured for native BSA in an aqueous buffer solution. Thus, the decrease in fluorescence lifetime is a clear consequence of the significant interaction between Re(I) complexes and BSA, with both the Trp 134 and Trp 212. The efficiency of lifetime quenching is found to be higher at Trp 212 (hydrophobic) which shows the stronger hydrophobic interaction between Re(I) complex and Trp 212 of BSA.

### 3.4. Conformational change of BSA in the presence of Re(I)-complex

The absorption and emission titration experiments confirm the interaction between Re(I) complexes and BSA. It is important to

Table 3  
Fluorescence resonance energy transfer (FRET) data for complexes **1a** and **1b** with Trp of BSA.

Complex	$J$ value/ $10^{-14}$ ( $\text{cm}^3 \text{ mol/L}$ )	$R_0$ (nm)	$E$	$r$ (nm)
<b>1a</b>	6.56	3.49	0.75	3.05
<b>1b</b>	1.39	2.69	0.85	2.16

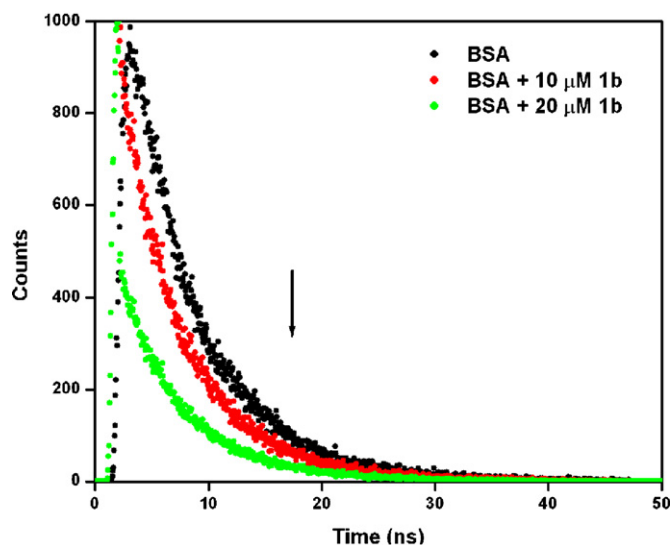


Fig. 6. Fluorescence decay curve of BSA in the presence of complex **1b**,  $[BSA] = 1 \times 10^{-5}$  M.

examine how the structure of BSA is affected in the presence of Re(I) complexes. When probes bind to a globular protein, the intramolecular forces responsible for maintaining the secondary and tertiary structures can be altered, resulting in a conformational change of the protein [50]. Circular dichroism is a sensitive technique to monitor conformational changes of protein upon interaction with small molecules. BSA has a high percentage of  $\alpha$ -helical structure which shows characteristic strong double minima signals at 208 and 222 nm (Fig. 7). The reasonable explanation is that the negative peaks at 208 and 222 nm are both contributed to  $n-\pi^*$  transition of the carbonyl group of peptide. The CD result is expressed as MRE (Mean Residue Ellipticity) in  $^\circ \text{cm}^2 \text{dmol}^{-1}$ , which is defined as Eq. (6).

$$\text{MRE} = \frac{\theta_{\text{obs}}}{10nlC_p} \quad (6)$$

Here  $\theta_{\text{obs}}$  is the CD in milli-degree,  $n$  is the number of amino acid residues (583),  $l$  is the path length of the cell (5 mm) and  $C_p$  is

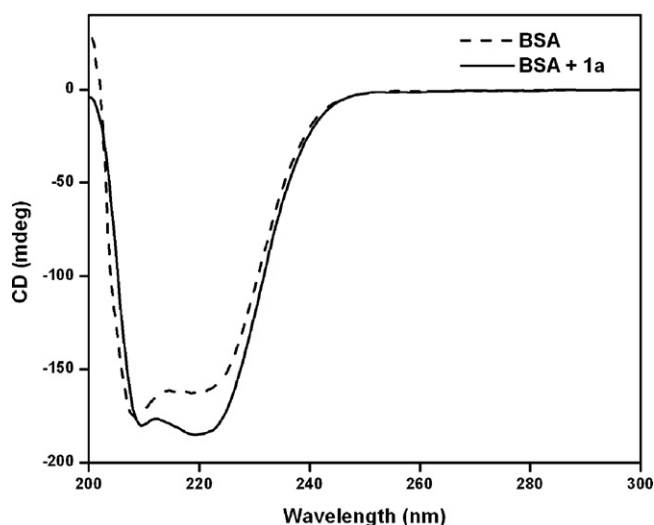


Fig. 7. CD spectra of BSA in the presence and absence of the complex **1a**,  $[BSA] = 3 \times 10^{-6}$  M and  $[1a] = 1 \times 10^{-5}$  M.

the mole fraction. The helical content is calculated from the MRE values at 208 nm using the Eq. (7) [51].

$$\alpha\text{-helix} = \left[ \frac{(-\text{MRE}_{208 \text{ nm}}) - 4000}{33,000 - 4000} \right] \times 100\% \quad (7)$$

In Eq. (7)  $\text{MRE}_{208 \text{ nm}}$  is the observed MRE value at 208 nm, 4000 is the MRE of the  $\beta$ -form and random coil conformation cross at 208 nm, and 33,000 is the MRE value of a pure  $\alpha$ -helical at 208 nm. The quantitative analysis of the CD data using Eq. (7) provides the  $\alpha$ -helix content in the secondary structure of serum albumin. The  $\theta$  value decreased on the addition of Re(I) complex with slight red shift, which is indicative of the loss of  $\alpha$ -helicity. Upon addition of Re(I) complexes to BSA the extent of  $\alpha$ -helicity of the protein decreases from 62% to 54% and 52% for complexes **1a** and **1b**, respectively. It is apparent that the Re(I) complexes (**1a** and **1b**) bind to the amino acid residues of the main polypeptide chain of BSA and destroy the hydrogen bonding networks present in the amino acid residues of protein which may decrease the percentage of  $\alpha$ -helicity of the protein [52]. Therefore, we can conclude that the effect of Re(I) complex on BSA causes a conformational change of the protein with the loss of  $\alpha$ -helix stability.

#### 4. Conclusions

The binding of Re(I)-complexes (**1a** and **1b**) with BSA is investigated using UV-visible, steady-state fluorescence, CD and fluorescence lifetime measurements. The BSA fluorescence exhibits an appreciable blue shift along with fluorescence intensity quenching and a decrease in the fluorescence lifetime upon binding with the Re(I) complexes. The decrease in both  $\tau_1$  and  $\tau_2$  values of BSA in the presence of Re(I) complexes show the interaction of probe with both Trp 134 and Trp 212 residues but stronger with the more hydrophobic Trp 212 residue. Quenching of BSA fluorescence and an enhancement in the Re(I) luminescence is found to be a function of the extent of spectral overlap between the donor's fluorescence and acceptor's absorption spectrum. This observation indicates that the energy transfer from the Trp residues of BSA to the probe, Re(I) complex occurs efficiently.

#### Acknowledgements

Financial support for this work from Rajiv Gandhi National Fellowship (UGC) is greatly acknowledged. SR thanks DST, New Delhi and Madurai Kamaraj University (UGC-UPE) for funding.

#### Appendix A. Supplementary data

Supplementary data associated with this article can be found, in the online version, at doi:10.1016/j.jphotochem.2011.10.022.

#### References

- [1] S.S. Sun, A.J. Lees, Transition metal based supramolecular systems: synthesis, photophysics, photochemistry and their potential applications as luminescent anion chemosensors, *Coord. Chem. Rev.* 230 (2002) 171–192.
- [2] D. Beck, J. Brewer, J. Lee, D. McGraw, B.A. DeGraff, J.N. Demas, Localizing molecular probes: inclusion of Re(I) complexes in  $\beta$ -cyclodextrin, *Coord. Chem. Rev.* 251 (2007) 546–553.
- [3] K.K.-W. Lo, M.-W. Louie, K.Y. Zhang, Design of luminescent iridium(III) and rhenium(I) polypyridine complexes as in vitro and in vivo ion, molecular and biological probes, *Coord. Chem. Rev.* 254 (2010) 2603–2622.
- [4] R.A. Kirgan, B.P. Sullivan, D.P. Rillema, Photochemistry and photophysics of coordination compounds: rhenium, *Top. Curr. Chem.* 281 (2007) 45–100.
- [5] M. Wrighton, D.L. Morse, The nature of the lowest excited state in tricarbonylchloro-1,10-phenanthroline-rhenium(I) and related complexes, *J. Am. Chem. Soc.* 96 (1974) 998–1003.
- [6] A. Juris, S. Campagna, I. Bidd, J.M. Lehn, R. Ziessel, Synthesis and photo-physical and electrochemical properties of new halotricarbonyl (polypyridine)rhenium(I) complexes, *Inorg. Chem.* 27 (1988) 4007–4011.

- [7] D.R. Cary, N.P. Zaitseva, K. Gray, K.E. O'Day, C.B. Darrow, S.M. Lane, T.A. Peyser, J.H. Satcher Jr., W.P. Van Antwerp, A.J. Nelson, J.G. Reynolds, Rhenium bipyridine complexes for the recognition of glucose, *Inorg. Chem.* 41 (2002) 1662–1669.
- [8] L.A. Mullice, S.J.A. Pope, The development of responsive, luminescent lifetime probes based upon axially functionalised *fac*-[Re(CO)<sub>3</sub>(di-imine)(L)]<sup>+</sup> complexes, *Dalton Trans.* 39 (2010) 5908–5917.
- [9] A.J. Amoroso, M.P. Coogan, J.E. Dunne, V.F. Moreira, J.B. Hess, A.J. Hayes, D. Lloyd, C. Millet, S.J.A. Pope, C. Williams, Rhenium *fac*-tricarboxyl bisimine complexes: biologically useful fluorochromes for cell imaging applications, *Chem. Commun.* (2007) 3066–3068.
- [10] H.D. Stoeffler, N.B. Thornton, S.L. Temkin, K.S. Schanze, Unusual photophysics of a rhenium(I) dipyrrophenazine complex in homogenous solution and bound to DNA, *J. Am. Chem. Soc.* 117 (1995) 7119–7128.
- [11] V.W.-W. Yam, K.K.-W. Lo, K.-K. Cheung, R.Y.-C. Kong, Deoxyribonucleic acid binding and photocleavage studies of rhenium(I) dipyrrophenazine complexes, *J. Chem. Soc. Dalton Trans.* (1997) 2067–2072.
- [12] V. Fernandez-Moreira, F.L. Thorp-Greenwood, M.P. Coogan, Application of d<sup>6</sup> transition metal complexes in fluorescence cell imaging, *Chem. Commun.* 46 (2010) 186–202.
- [13] E. Meggers, Targeting proteins with metal complexes, *Chem. Commun.* (2009) 1001–1010.
- [14] J. Maksimoska, L. Feng, K. Harms, C. Yi, J. Kissil, R. Marmorstein, E. Meggers, Targeting large kinase active site with rigid, bulky octahedral ruthenium complexes, *J. Am. Chem. Soc.* 130 (2008) 15764–15765.
- [15] S.P. Mulcahy, E. Meggers, Organometallics as structural scaffolds for enzyme inhibitor design, *Top. Organomet. Chem.* 32 (2010) 141–153.
- [16] C.L. Davies, E.L. Dux, A.-K. Duhme-Klair, Supramolecular interactions between functional metal complexes and proteins, *Dalton Trans.* (2009) 10141–10154.
- [17] C. Liu, H. Xu, The metal site as a template for the metalloprotein structure formation, *J. Inorg. Biochem.* 88 (2002) 77–86.
- [18] N. Shahabadi, M. Maghsudi, Binding studies of a new copper (II) complex containing mixed aliphatic and aromatic dinitrogen ligands with bovine serum albumin using different instrumental methods, *J. Mol. Struct.* 929 (2009) 193–199.
- [19] V. Rajendiran, M. Palaniandavar, P. Swaminathan, L. Uma, Cleavage of proteins by a mixed-ligand copper(II) phenolate complex: hydrophobicity of the diimine coligand promotes cleavage, *Inorg. Chem.* 46 (2007) 10446–10448.
- [20] K.K.-W. Lo, K.-S. Sze, K.H.-K. Tsang, N. Zhu, Luminescent tricarboxylrhenium(I) dipyrroquinoxaline indole complexes as sensitive probes for indole-binding proteins, *Organometallics* 26 (2007) 3440–3447.
- [21] K.K.-W. Lo, K.H.-K. Tsang, W.-K. Hui, N. Zhu, Synthesis, characterization, crystal structure, and electrochemical, photophysical, and protein-binding properties of luminescent rhenium(I) diimine indole complexes, *Inorg. Chem.* 44 (2005) 6100–6110.
- [22] J.F. Foster, V.M. Rosener, M. Oratz, M.A. Rothschild (Eds.), *In Albumin Structure, Function and Uses*, Pergamon Press Inc., Oxford, UK, 1977.
- [23] T. Peters Jr., Serum albumin, *Adv. Protein Chem.* 37 (1985) 161–245.
- [24] N. Zhou, Y.Z. Liang, P. Wang, 18β-Glycyrrhetic acid interaction with bovine serum albumin, *J. Photochem. Photobiol. A* 185 (2007) 271–276.
- [25] L. Shang, X. Jiang, S. Dong, In vitro study on the binding of neutral red to bovine serum albumin by molecular spectroscopy, *J. Photochem. Photobiol. A* 184 (2006) 93–97.
- [26] M.N. Jones, Surfactant interactions with biomembranes and proteins, *Chem. Soc. Rev.* 21 (1992) 127–136.
- [27] K. Takeda, K. Hachiya, Y. Moriyama, *Interaction of Protein with Ionic Surfactants, Part 2*, Marcel Dekker, New York, 2002.
- [28] E.W. Abel, G. Wilkinson, Carbonyl halides of manganese and some related compounds, *J. Chem. Soc.* (1959) 1501–1505.
- [29] K.K.W. Lo, K.H.K. Tsang, N. Zhu, Luminescent tricarboxylrhenium(I) polypyridine estradiol conjugates: synthesis, crystal structure, and photophysical, electrochemical, and protein-binding properties, *Organometallics* 25 (2006) 3220–3227.
- [30] P. Bourassa, C.D. Kanakis, P. Tarantilis, M.G. Pollissiou, H.A. Tajmir-Riahi, Resveratrol, genistein, and curcumin bind bovine serum albumin, *J. Phys. Chem. B* 114 (2010) 3348–3354.
- [31] J.R. Lakowicz, *Principles of Fluorescence Spectroscopy*, 3rd ed., Plenum, New York, 2006.
- [32] Y. Shen, B.P. Maliwal, J.R. Lakowicz, Long-lived luminescent Re(I) complexes containing cis-carbonyl and bidentate phosphine ligands, *J. Fluoresc.* 11 (2001) 315–318.
- [33] P.J. Giordano, M.S. Wrighton, The nature of the lowest excited state in *fac*-tricarboxylhalobis(4-phenylpyridine)rhenium(I) and *fac*-tricarboxylhalobis(4,4'-bipyridine)rhenium(I): emissive organometallic complexes in fluid solution, *J. Am. Chem. Soc.* 101 (1979) 2888–2897.
- [34] K.K.W. Lo, M.W. Louie, K. Shing Sze, J.S.Y. Lau, Rhenium(I) polypyridine biotin isothiocyanate complexes as the first luminescent biotinylation reagents: synthesis, photophysical properties, biological labeling, cytotoxicity, and imaging studies, *Inorg. Chem.* 47 (2008) 602–611.
- [35] D.B. Wetlaufer, Ultraviolet spectra of proteins and amino acids, *Adv. Protein Chem.* 17 (1963) 303–390.
- [36] B.K. Paul, A. Samanta, N. Guchhait, Exploring hydrophobic subdomain IIA of the protein bovine serum albumin in the native, intermediate, unfolded, and refolded states by a small fluorescence molecular reporter, *J. Phys. Chem. B* 114 (2010) 6183–6196.
- [37] W.R. Ware, Oxygen quenching of fluorescence in solution: an experimental study of the diffusion process, *J. Phys. Chem.* 66 (1962) 455–458.
- [38] R. Flehr, A. Kienzler, W. Bannwarth, M.U. Kumke, Photophysical characterization of a FRET system using tailor-made DNA oligonucleotide sequences, *Bioconjugate Chem.* 21 (2010) 2347–2354.
- [39] M.J. Li, W.M. Kwok, W.H. Lam, C.H. Tao, V.W.W. Yam, D.L. Phillips, Synthesis of coumarin-appended pyridyl tricarboxylrhenium(I) 2,2'-bipyridyl complexes with oligoether spacer and their fluorescence resonance energy transfer studies, *Organometallics* 28 (2009) 1620–1630.
- [40] D. Zhao, J. Du, Y. Chen, X. Ji, Z. He, W.H. Chan, A quencher-tether-ligand probe and its application in biosensor based on conjugated polymer, *Macromolecules* 41 (2008) 5373–5378.
- [41] M. Klajner, P. Hebraud, C. Sirlin, C. Gaiddon, S. Harlepp, DNA binding to an anticancer organo-ruthenium complex, *J. Phys. Chem. B* 114 (2010) 14041–14047.
- [42] X.-F. Zhang, L. Xie, Y. Liu, J.-F. Xiang, L. Li, Y.-L. Tang, Molecular interaction and energy transfer between human serum albumin and bioactive component Aloe dihydrocoumarin, *J. Mol. Struct.* 888 (2008) 145–151.
- [43] T. Forster, O. Sinanoglu (Eds.), *Modern Quantum Chemistry*, vol. 3, Academic Press, New York, 1996.
- [44] S.M.T. Shaikh, J. Seetharamappa, P.B. Kandagal, S. Ashoka, Binding of the bioactive component isothipendyl hydrochloride with bovine serum albumin, *J. Mol. Struct.* 786 (2006) 46–52.
- [45] B. Valeur, J.C. Brochon, *New Trends in Fluorescence Spectroscopy*, 6th ed., Springer Press, Berlin, 1999.
- [46] P. Das, A. Mallick, B. Haldar, A. Chakrabarty, N. Chattopadhyay, Effect of nanocavity confinement on the rotational relaxation dynamics: 3-acetyl-4-oxo-6,7-dihydro-12H indolo-[2,3-a]quinolizine in micelles, *J. Chem. Phys.* 125 (2006), 044516-1–044516-6.
- [47] A. Mallick, B. Haldar, N. Chattopadhyay, Spectroscopic investigation on the interaction of ICT probe 3-acetyl-4-oxo-6,7-dihydro-12H Indolo-[2,3-a] quinolizine with serum albumins, *J. Phys. Chem. B* 109 (2005) 14683–14690.
- [48] A.B. Patel, S. Srivastava, R.S. Phadke, Interaction of 7-hydroxy-8-(phenylazo)1,3-naphthalenedisulfonate with bovine plasma albumin. Spectroscopic studies, *J. Biol. Chem.* 274 (1999) 21755–21762.
- [49] B. Ojha, G. Das, The interaction of 5-(alkoxy)naphthalen-1-amine with bovine serum albumin and its effect on the conformation of protein, *J. Phys. Chem. B* 114 (2010) 3979–3986.
- [50] U.K. Hansen, Molecular aspects of ligand binding to serum albumin, *Pharmacol. Rev.* 33 (1981) 17–53.
- [51] N. Greenfield, G.D. Fasman, Computed circular dichroism spectra for the evaluation of protein conformation, *Biochemistry* 8 (1969) 4108–4116.
- [52] S.M.T. Shaikh, J. Seetharamappa, P.B. Kandagal, D.H. Manjunatha, S. Ashoka, Spectroscopic investigations on the mechanism of interaction of bioactive dye with bovine serum albumin, *Dyes Pigments* 74 (2007) 665–671.